TRANSFORMER SYMPATHETIC INRUSH CURRENT IDENTIFICATION CRITERION BASED ON THE VARIATION CHARACTERISTICS OF NON-PERIODIC COMPONENTS

Zhendong LI[1], Haiwang JIN[1], Chuanyu SUN[2], Jinbo LI[1,3], Shuangming DUAN[2*]

The protection will be disactivated because the second harmonic content of the differential current is less than the fixed value following the temporary saturation of the current transformer (CT) caused by the non-periodic component of the transformer sympathetic inrush current. However, when the transformer has turn-to-turn faults, the second harmonic content of the differential current is higher than the customized one, resulting in differential protection refusal. These issues are used to analyze the transformer differential protection misoperation behavior, study the mechanism of the transformer sympathetic inrush current and how it differs from fault current, and identify the slow change of the non-periodic component when sympathetic inrush current occurs in the transformer. Furthermore, to prevent maloperation when the CT is saturated, an identification criterion based on variations in the aperiodic component has been incorporated. As an addition to the conventional differential protection, a complete set of identification methods for sympathetic inrush current based on the change of nonperiodic components is further constructed. PSCAD/EMTDC simulation is used to confirm the suggested method's efficacy.

Keywords: transformer differential protection; current transformer (CT) saturation; sympathetic inrush; inter-turn failure; second harmonic braking; nonperiodic component

1. Introduction

Transformer in the power system occupies a pivotal position, according to the working principle of the transformer and equipment material characteristics can be known, the transformer for no-load closing with a high probability of generating magnetizing inrush current, the inrush current will also make the normal operation of the transformer connected in parallel with the transformer and should be sympathetic inrush current phenomena[1-5], As early as 1941, Hayward discovered

[1] State Grid Jibei Electric Power Co., Ltd. UHV Branch, Beijing 102488, China
[2] Key Laboratory of Modern Power System Simulation and Control & Renewable Energy Technology, Ministry of Education, Northeast Electric Power University, Jilin 132012, China,
[3] Hebei Key Laboratory of Equipment and Technology Demonstration of Flexible DC Transmission, Tianjin 300100, China
* Corresponding author: Shuangming Duan, E-mail: duansm@neepu.edu.cn

this phenomenon through field fault recordings, pointing out that the decay period of this surge was long [6]. Bronzeado et al. further analyzed that the sympathetic inrush current is generated due to the coupling of the magnetizing inrush current with the impedance parameter of the system, which makes the terminal voltage of the operating transformer to be shifted, through the expression of the flux linkage of the shunt transformer and called this coupling process as the sympathetic interaction [7]. The DC component of the sympathetic inrush current that decays slowly can easily lead to local transient saturation of the current transformer, which makes the second harmonic criterion of the differential current invalid and leads to the differential protection not being able to block correctly [8-10]. In addition, the problem of distinguishing between sympathetic inrush current and short-circuit current has been a research hotspot of differential protection [11-13].

A study of how sympathetic inrush currents are generated and their changing characteristics. In [14], the attenuation mechanism of sympathetic inrush current is studied in depth from the point of view of iron core bias, and it is pointed out that the system resistance plays the main attenuation role in the inrush current at the initial stage, and as the inrush current evolves, it is only possible to attenuate the bias magnetism by virtue of the transformer's own resistance. The generation principle of sympathetic inrush current is analyzed in [15] and a model of sympathetic inrush current in shunt transformer is constructed using PSCAD software. To analyze the characteristics of the sympathetic inrush current, it is necessary to derive the analytical equation of the transformer flux linkage and analyze the change rule of the sympathetic inrush current.

For the identification study of sympathetic inrush current, An artificial neural network approach was used in [16] to improve the protection of a double-winding transformer, so that it is able to recognize and sympathetic inrush current, but the ability to recognize it accurately in real operating conditions is a great test. The method proposed in [17] is capable of accurately recognizing and sympathetic inrush current and short-circuit faults, but is susceptible to CT saturation affecting its performance. Three differentiated criteria are proposed in [18] to identify and sympathetic inrush current, but they are computationally intensive and susceptible in practical operation. The estimation of flux identification and sympathetic inrush current by integrating the voltage on the transformer side is proposed in [19], but there are many influencing factors, which make it difficult to differentiate during the actual operation.

Currently, transformer differential protection uses traditional excitation inrush identification methods such as second harmonic braking to identify and sympathetic inrush current. However, the inrush current waveforms and attenuation change characteristics in different cases are very different, especially affected by CT saturation. At the same time, the second harmonic content of turn-to-turn short circuit may also exceed the braking factor, which may cause the false operation of

differential protection. In this paper, the transformer and sympathetic inrush current mechanism and change characteristics are sorted out, and the transformer differential protection misoperation is analyzed. In addition, based on the time-domain change characteristics of the non-periodic component of the differential current, a new identification method of the sympathetic inrush current is proposed. The method has a small computational amount and can quickly and reliably recognize sympathetic inrush current and take corresponding braking measures. The effectiveness and feasibility of the method are verified by simulation tests.

2. Mechanism and change characteristics of transformer sympathetic inrush current

Transformers coupled in series or parallel commonly generate sympathetic inrush current; parallel transformers are more frequently found in substations, while series transformers are typically employed in step-down distribution systems. Since the parallel transformer model and the series transformer circuit model used to examine the sympathetic interaction between the transformer derivation process are comparable, the subject of this paper is the parallel transformer generated sympathetic inrush current, which happens when equivalent circuit Fig. 1 depicts the comparable circuit in the event of sympathetic inrush current.

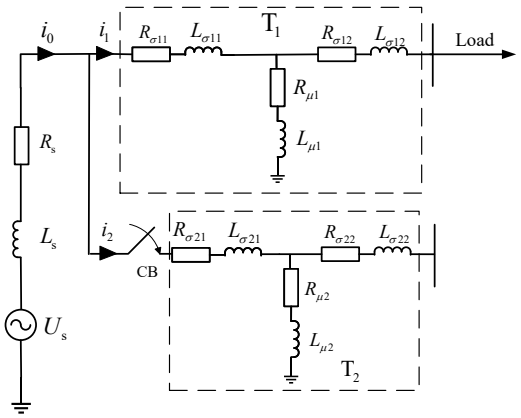

Fig. 1 Equivalent circuit of parallel transformers

where T_1 is the operating transformer, T_2 is the transformer with no-load cl osing, and CB is the circuit breaker. U_s, L_s, R_s, i_s are the system-side voltage, equiv alent inductance, equivalent resistance and current. $R_{\sigma 11}$, $L_{\sigma 11}$, $R_{\sigma 12}$, $L_{\sigma 12}$ are the wi nding resistance and leakage inductance of the primary and secondary sides of T_1. $R_{\mu 1}$, $L_{\mu 1}$ are the magnetic resistance and magnetic inductance of T_1, $R_{\sigma 21}$, $L_{\sigma 21}$, $R_{\sigma 2 2}$, $L_{\sigma 22}$ are the winding resistance and leakage inductance of the primary and secon dary sides of T_2. $R_{\mu 2}$, $L_{\mu 2}$ are the magnetic resistance and magnetic inductance of T $_2$. i_1 and i_2 are the currents on the T_1 and T_2 sides. Operating transformers in substa

tions are often linked to passive loads, which merely alter the sympathetic inrush current's amplitude. The T_1 side loads are disregarded in order to better examine and react to inrush current phenomena. Consequently, in the equivalent model, the transformer secondary winding is negligible because there is no load, and the leakage inductance is also negligible in comparison to the magnetizing inductance,it means $L_{\sigma 11}=L_{\sigma 21}=0$. Furthermore let $R_1=R_{\sigma 11}+R_{\mu 1}$, $R_2=R_{\sigma 21}+R_{\mu 2}$, $L_1=L_{\mu 1}$, $L_2=L_{\mu 2}$.According to Kirchhoff's law, when t=0, CB is closed and gets

$$\begin{cases} U_{\mathrm{m}}\sin(\omega t+\varphi)=R_{\mathrm{s}}i_0(t)+L_{\mathrm{s}}\dfrac{di_0(t)}{dt}+R_1i_1(t)+\dfrac{d\psi_1(t)}{dt} \\ U_{\mathrm{m}}\sin(\omega t+\varphi)=R_{\mathrm{s}}i_0(t)+L_{\mathrm{s}}\dfrac{di_0(t)}{dt}+R_2i_2(t)+\dfrac{d\psi_2(t)}{dt} \\ i_0(t)=i_1(t)+i_2(t) \end{cases} \tag{1}$$

Where $\psi_1(t)$ and $\psi_2(t)$ are the flux linkage of T_1 and T_2. Meanwhile, the equivalent magnetizing branch of the transformer core is taken as the average inductance[20]. It means $i_1(t)=\psi_1(t)/L_{\mu 1}$, $i_2(t)=\psi_2(t)/L_{\mu 2}$, The Laplace transform of Eq. (1) gives the equations for the two transformer magnetic chains $\psi_1(t)$ and $\psi_2(t)$ at this time

$$\begin{cases} \psi_1=a_1\sin\left(\omega t+\varphi+\theta_1+\gamma_1+\gamma_2\right)+b_1e^{\tau_1 t}+c_1e^{\tau_2 t} \\ \psi_2=a_2\sin\left(\omega t+\varphi+\theta_2+\gamma_1+\gamma_2\right)+b_2e^{\tau_1 t}+c_2e^{\tau_2 t} \end{cases} \tag{2}$$

The coefficients in Eq.(2) are

$$\begin{cases} a_1=\dfrac{-U_mL_1\sqrt{\left(R_2^2+L_2^2\omega^2\right)\left[\left(a\omega^2-c\right)^2+b^2\omega^2\right]}}{a^2\left(\tau_1^{\,2}+\omega^2\right)\left(\tau_2^{\,2}+\omega^2\right)} \\ a_2=\dfrac{-U_mL_2\sqrt{\left(R_1^2+L_1^2\omega^2\right)\left[\left(a\omega^2-c\right)^2+b^2\omega^2\right]}}{a^2\left(\tau_1^{\,2}+\omega^2\right)\left(\tau_2^{\,2}+\omega^2\right)} \end{cases} \tag{3}$$

$$\begin{cases} b_1=\dfrac{L_1}{\sqrt{b^2-4ac}}\left\{(R_{\mathrm{s}}+\tau_1L_{\mathrm{s}})\left[\psi_1(0)-\psi_2(0)\right]\right. \\ \qquad \left.+(R_2+\tau_1L_2)\left[\dfrac{U_m\omega}{(\tau_1^{\,2}+\omega^2)}+\dfrac{L_{\mathrm{s}}}{L_2}\psi_2(0)+\dfrac{L_1+L_{\mathrm{s}}}{L_1}\psi_1(0)\right]\right\} \\ b_2=\dfrac{L_1}{\sqrt{b^2-4ac}}\left\{(R_{\mathrm{s}}+\tau_2L_{\mathrm{s}})\left[\psi_1(0)-\psi_2(0)\right]\right. \\ \qquad \left.+(R_2+\tau_2L_2)\left[\dfrac{U_m\omega}{(\tau_2^{\,2}+\omega^2)}+\dfrac{L_{\mathrm{s}}}{L_2}\psi_2(0)+\dfrac{L_1+L_{\mathrm{s}}}{L_1}\psi_1(0)\right]\right\} \end{cases} \tag{4}$$

$$\begin{cases} c_1 = \dfrac{L_1}{\sqrt{b^2-4ac}}\Big\{(R_s+\tau_2 L_s)\big[\psi_1(0)-\psi_2(0)\big] \\ \qquad +(R_2+\tau_2 L_2)\left[\dfrac{U_m\omega}{(\tau_2{}^2+\omega^2)}+\dfrac{L_s}{L_2}\psi_2(0)+\dfrac{L_1+L_s}{L_1}\psi_1(0)\right]\Big\} \\ c_2 = \dfrac{L_2}{\sqrt{b^2-4ac}}\Big\{(R_s+\tau_2 L_s)\big[\psi_2(0)-\psi_1(0)\big] \\ \qquad +(R_1+\tau_2 L_1)\left[\dfrac{U_m\omega}{(\tau_2{}^2+\omega^2)}+\dfrac{L_s}{L_1}\psi_1(0)+\dfrac{L_2+L_s}{L_2}\psi_2(0)\right]\Big\} \end{cases} \tag{5}$$

Where $\psi_1(0)$ and $\psi_2(0)$ are the residual magnetism of the two transformers when T_2 is closed. $a=L_1L_2+L_2L_s+L_sL_1$, $c=R_sR_2+R_sR_1+R_1R_2$, $b=L_1R_s+R_1L_s+R_2L_1+R_1L_2+R_2L_s+L_1R_2$, $\tau_1=[-b+(b^2-4ac)^{1/2}]/2a$, $\tau_2=[-b-(b^2-4ac)^{1/2}]/2a$. $\theta_1=\arctan(\omega L_2/R_2)$, $\theta_2=\arctan(\omega L_2/R_2)$, $\gamma_1=\arctan(\omega/\tau_1)$, $\gamma_2=\arctan(\omega/\tau_2)$. During the actual operation process, the parameters of the parallel transformers tend to be identical. It means $R_1=R_2=R$, $L_1=L_2=L$. The time-domain expressions for the magnetizing inrush current and the sympathetic inrush current can be derived as

$$\begin{cases} i_1(t) = a_3\sin(\omega t+\varphi+\alpha)+b_3e^{\tau_3 t}-c_3e^{\tau_4 t} \\ i_2(t) = a_3\sin(\omega t+\varphi+\alpha)+b_3e^{\tau_3 t}+c_3e^{\tau_4 t} \end{cases} \tag{6}$$

The coefficients in Eq.(6) are

$$\begin{cases} a_3 = \dfrac{U}{\sqrt{(R+2R_s)^2+(\omega L+2\omega L_s)^2}} \\ b_3 = \dfrac{1}{2L}\left[-\dfrac{2L}{\sqrt{(R+2R_s)^2+(\omega L+2\omega L_s)^2}}U_m\sin(\theta+\alpha)+\psi_1(0)+\psi_2(0)\right] \\ c_3 = \dfrac{1}{2L}[\psi_1(0)-\psi_2(0)] \end{cases} \tag{7}$$

Where $\alpha=-\arctan[\omega(L+L_s)/(R+R_s)]$, $\tau_3=-(R+2R_s)/(L+2L_s)$, $\tau_4=-R/L$. Eq. (2) and (6) demonstrate that the flux linkage and inrush current of the two transformers are made up of three parts: two decaying non-periodic components and one sinusoidal steady state component. Describe the non-periodic elements of the two transformers' inrush current and flux linkage as

$$\begin{cases} \psi_{1DC} = b_1e^{\tau_1 t}+c_1e^{\tau_2 t} \\ \psi_{2DC} = b_2e^{\tau_1 t}+c_2e^{\tau_2 t} \\ i_{1DC} = b_3e^{\tau_3 t}-c_3e^{\tau_4 t} \\ i_{1DC} = b_3e^{\tau_3 t}+c_3e^{\tau_4 t} \end{cases} \tag{8}$$

The variation of the non-periodic components of the magnetic chain and th e inrush current is obtained as an example for a set of typical transformer parameters as shown in Fig. 2

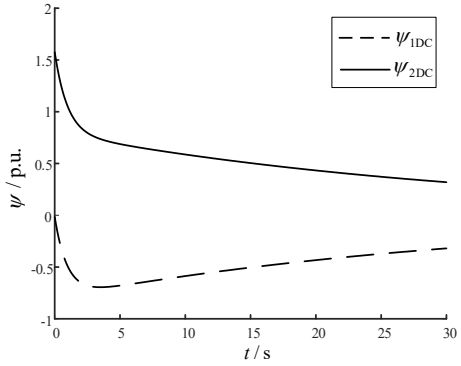

(a) Non-periodic component of the flux linkage of the two transformers

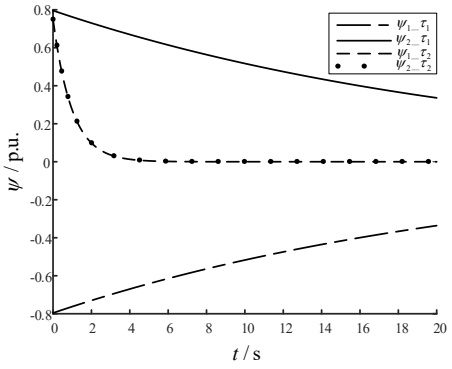

(b) Non-periodic components of the two transformer flux linkage contain components of τ_1 and τ_2

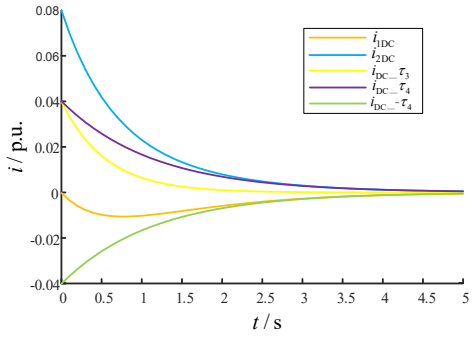

(c) Non-periodic component of two transformer inrush currents

Fig. 2 Non-periodic component curve of transformer flux linkage and inrush current

By combining the curves with Eq. (2) and (6), a quick examination of the sympathetic inrush current and flux linkage change patterns yields the following findings:

1) Since $a\omega^2$-c>>b, the amplitude and phase magnitude of the periodic components of T_1 and T_2 are the same and are not affected by changes in the equivalent parameters of the system.

(2) As illustrated in Fig. 2, sympathetic inrush current is produced by the combined action of the flux linkage sinusoidal steady state component and nonperiodic component. In Fig. 2(a) $\psi_1(t)$ and $\psi_2(t)$, the two nonperiodic components of the transformer flux connection, have opposing polarity. After some time of closing the gate, the non-periodic component ψ_{1DC} of the running transformer flux linkage $\psi_1(t)$ rises to a high value and then gradually falls. After closure, the non-periodic component ψ_{2DC} of the no-load closing transformer flux linkage $\psi_2(t)$ quickly peaks and then progressively declines. sympathetic inrush current The sympathetic interaction between the unloaded transformer and the running transformer reduces the inrush's rate of decay after the sympathetic inrush current appears.

(3) The two parts of the free components in the no-load-closing transformer ψ_{2DC} have the same polarity, so the polarity of the ψ_{2DC} does not change and continues to decay, even though the two parts of the non-periodic components of the flux linkage of the two transformers have the same decay coefficients of the two free components, both τ_1 and τ_2. However, the size and polarity of the two free components differ, leading to different phenomena in the flux linkage change process. The polarity of ψ_{2DC} remains constant and keeps declining. The two free components in the working transformer, ψ_{1DC}, have opposing polarities. However, because of the flux linkage, which prevents abrupt changes, ψ_{1DC} is zero when the switch is off. Since the free component of positive polarity changes more quickly than that of negative polarity after the switch is on, ψ_{1DC} has negative polarity and its amplitude rises. At the same time, the rate at which the free component of positive polarity changes gradually falls, below that of negative polarity, and the amplitude of ψ_{1DC} begins to fall.

3. Differential Protection Malfunction Analysis

Differential protection is designed according to KCL as the basic principle, Fig. 3 shows the principle diagram of differential protection for double winding transformer, I_1 and I_2 are the primary and secondary side currents, respectively, I_1' and I_2' are the currents after CT transmission, respectively, and $I_d = I_1' + I_2'$ is the differential current.

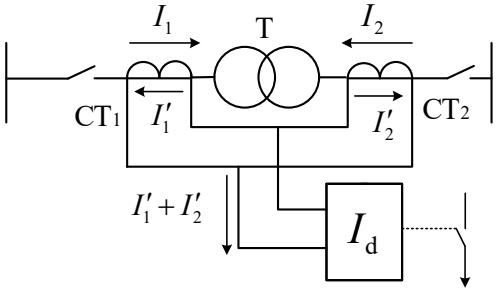

Fig. 3 Wiring diagram of transformer differential protection principle

The action criterion of the differential protection is as shown in Eq.9.

$$\begin{cases} I_d > I_{dset} & I_{res} \le I_{res.0} \\ I_d > K(I_{res} - I_{res.0}) + I_{dset} & I_{res} > I_{res.0} \end{cases} \tag{9}$$

Where, I_{dset} is the action of the rectification value, I_{res} is the braking current value, $I_{res.0}$ is the inflection point of the braking characteristics, K is the braking characteristic slope, often between 0.5 and 1. It is conceivable to cause the differential current to increase to a level that would activate the brake protective device threshold, which would initiate the unexpected protection action, in the event of transformer inrush. Since there is a high amplitude second harmonic component in the differential current during the inrush, a requirement for second harmonic braking is established using equation 10. When the differential current satisfies the conditions of equation 10, the protective device will recognise the inrush current and block the protection.

$$\frac{I_{d2}}{I_{d1}} .. K_{d,set} \tag{10}$$

Where I_{d2} is the second harmonic amplitude of the differential current, I_{d1} is the fundamental amplitude of the differential current, $K_{d,\ set}$ for the braking coefficient is usually taken as 15% ~ 20%.

3.1 Analysis of sympathetic inrush current second harmonic braking

Section 1 illustrates how the sympathetic interaction causes the operating t ransformer′s flux linkage to gradually become saturated after T_2 the gate closes. D uri-ng this phase, the excitation current increases, and the second harmonic conten t is high. In the desaturation stage, the excitation current decreases, and the differe nti-al protection can be precisely blocked by the second harmonic braking.

The non-periodic component of the sympathetic inrush current causes the current transformer to temporarily become saturated, which forces the current transformer to operate in the local hysteresis return region. This results in measurement errors for the differential current, which rises while the amplitude of

the second harmonic of the differential current falls, ultimately leading to the failure of the second harmonic braking.

The B-phase and C-phase differential currents are $I_{dB}=I_B-I_C-\eta I_b$ and $I_{dC}=I_C-I_A-\eta I_c$, respectively, as a result of the Yd11 transformer normalizing to one side to calculate the differential current. I_A, I_B, and I_C are the CT secondary currents on the transformer's main side, whereas I_a, I_b, and I_c are the CT secondary currents on the transformer's secondary side. The transformer ratio is denoted by η. According to the study above, a spurious two-phase differential current may be produced in the relay after the CT reaches the saturation phase as a result of non-periodic components causing a measurement error.

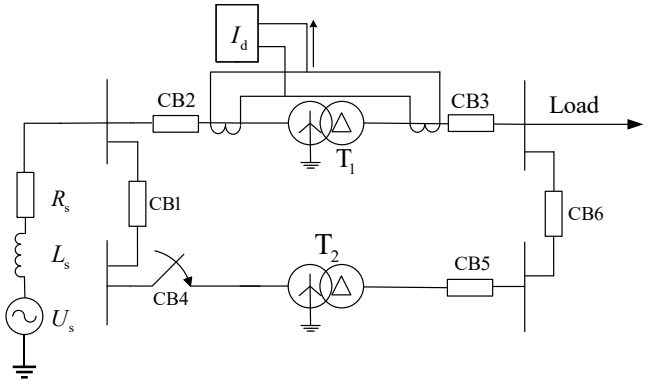

Fig. 4 Equivalent circuit of single-phase transformer

Taking the shunt transformer group as an example, the simulation model s hown in Fig. 4 is constructed, and the CT ratio of the Y-side of the operating trans former is 1:320, and the CT ratio of the Δ-side is 1:600. The windings on the seco ndary side of the two transformers are 0.5Ω. The second harmonic braking coeffic ient , $K_{d,\ set}$, is set to be 0.15. The second harmonic ratio change curve is obtained by no-load closing of T_2 at 0.2 s. The second harmonic ratio change curve is obtai ned from the differential current.

As it can be seen from Fig. 5, when CT is not saturated, the differential pro tection based on second harmonic braking can effectively recognize and sympathe tic inrush current and block the protection. However, after the CT is saturated, the second harmonic content in the differential current is lower than the braking coeffi cient after the sympathetic inrush current reaches the peak value, which leads to th e protection misoperation.

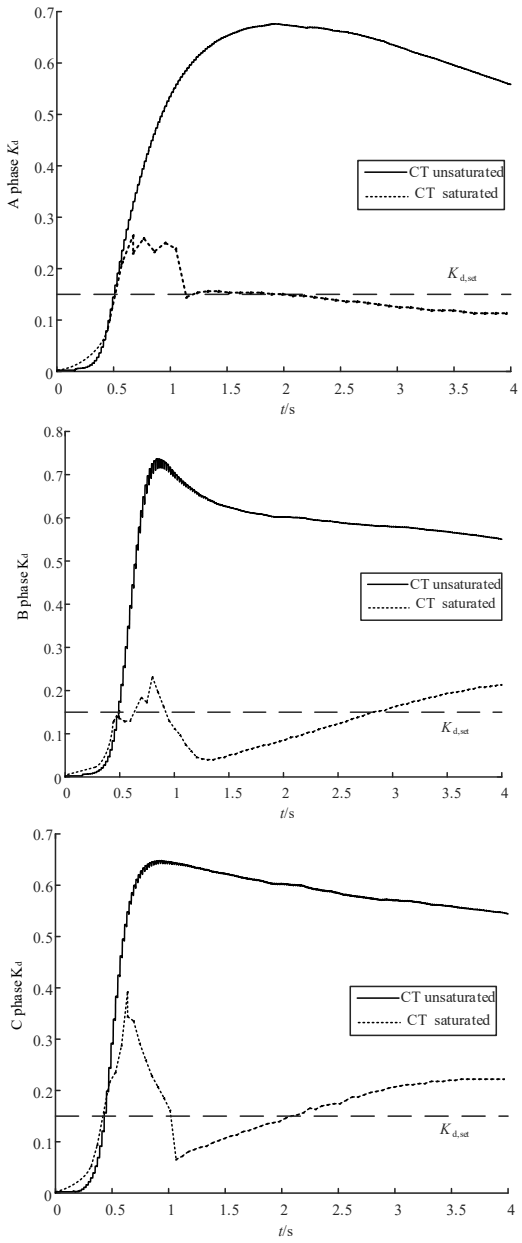

Fig. 5 The braking situation of second harmonic during sympathetic inrush current

3.2 Analysis of second harmonic braking in the event of a turn-to-turn short circuit in a transformer

At 0.2s, a slight turn-to-turn short-circuit is set to occur in phase A of the operating transformer T_1 with a ratio of 5%, and the second harmonic percentage of the three-phase differential current in the event of an internal transformer turn-to-turn short-circuit is shown in Fig. 6.

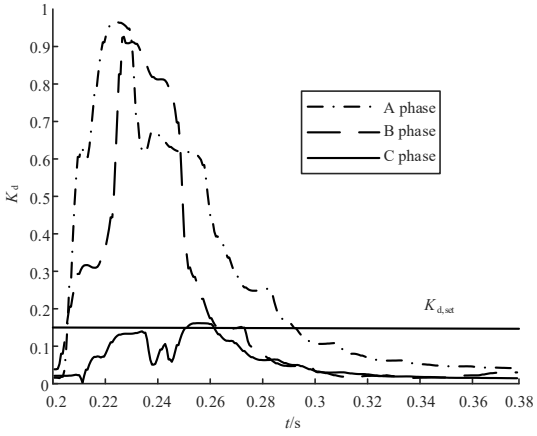

Fig. 6 The secondary harmonic braking condition when an inter-turn short circuit occurs inside the transformer

In the event of a slight inter-turn short circuit, phase A and B have a high percentage of second harmonics and Eq. 10 is continuously satisfied. The second harmonic braking action causes the differential protection to block for a long time.

4. Recognition method based on the characterization of non-periodic component changes

4.1Effect of Δ-side circulation and phase difference compensation on the rate of change of nonperiodic components

A single-phase transformer will be utilized as an example for in-depth research in order to streamline the procedure and investigate the fundamental ideas. When the equivalent circuit diagram, depicted in Fig. 7, is used, a single-phase transformer occurs sympathetic inrush current. In this diagram, the primary side of the transformer's resistance and leakage inductance is represented by $R_{\sigma 1}$, $L_{\sigma 1}$, the secondary side by $R_{\sigma 2}$, $L_{\sigma 2}$, and the excitation inductance by L_{μ}, excluding the excitation resistance.

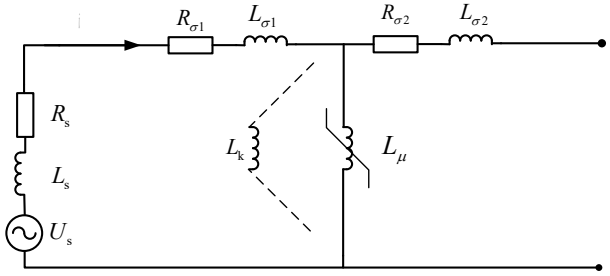

Fig. 7 Equivalent circuit of single-phase transformer

When a transformer turn-to-turn short circuit occurs, it can be regarded as a three-winding transformer short-circuited in the third winding, so the turn-to-turn

short circuit is equivalent to a short-circuited turn leakage reactance L_k connected in parallel on the excitation branch. by the can be listed separately and should be and should be and should be and should be and turn-to-turn short circuit when the attenuation constant τ and τ' equations.

$$\begin{cases} \tau = \dfrac{\left(L_s + L_{\sigma 1}\right) + L_\mu // L_{\sigma 2}}{R_s + R_{\sigma 1}} \\ \tau' = \dfrac{\left(L_s + L_{\sigma 1}\right) + L_\mu // L' // L_{\sigma 2}}{R_s + R_{\sigma 1} + R'} \end{cases} \tag{11}$$

The above single-phase transformer as an example, from the principle to analyze the transformer occurs and should be sympathetic inrush current and turn-to-turn short circuit when the current non-periodic component of the difference between the trend of change. As for the three-phase transformer, in addition to the three-phase symmetry of the excitation branch circuit, so it can be generalized to the three-phase transformer, the non-periodic component decays faster when a turn-to-turn short circuit occurs. But three-phase transformer three-phase excitation branch asymmetry, at this time the non-periodic component attenuation has what kind of law, need to be further discussed. Establish Fig. 8 as an example of transformer wiring diagram for analysis, three-phase transformer consists of three single-phase transformer.

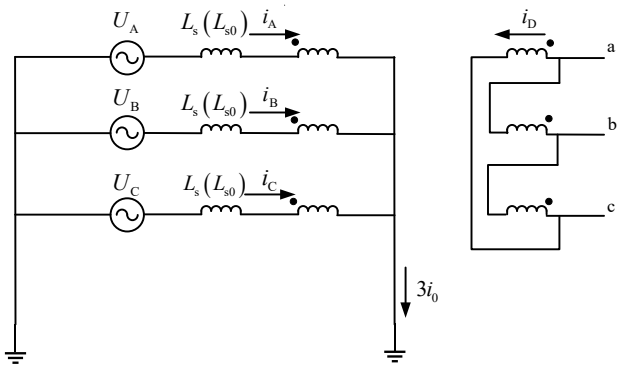

Fig. 8 Circuit of Yd11 connection transformer

Write and solve the equation for Fig. 8 and since the excitation branch current is the sum of the loop current and line current, the Δ-side loop current and primary side current can be found to be

$$i_\Delta = \frac{L_\sigma + L_{s0}}{3\left(L_\sigma + L_{\sigma\Delta} + L_{s0}\right)}\left(i_{\mu a} + i_{\mu b} + i_{\mu c}\right) \tag{12}$$

$$\begin{cases} i_{\mathrm{A}} = \dfrac{2L_{\sigma}+2L_{\mathrm{s0}}+3L_{\sigma\Delta}}{3\left(L_{\sigma}+L_{\mathrm{s0}}+L_{\sigma\Delta}\right)} i_{\mu\mathrm{a}} - \dfrac{L_{\sigma}+L_{\mathrm{s0}}}{3\left(L_{\sigma}+L_{\mathrm{s0}}+L_{\sigma\Delta}\right)}\left(i_{\mu\mathrm{b}}+i_{\mu\mathrm{c}}\right) \\ i_{\mathrm{B}} = \dfrac{2L_{\sigma}+2L_{\mathrm{s0}}+3L_{\sigma\Delta}}{3\left(L_{\sigma}+L_{\mathrm{s0}}+L_{\sigma\Delta}\right)} i_{\mu\mathrm{b}} - \dfrac{L_{\sigma}+L_{\mathrm{s0}}}{3\left(L_{\sigma}+L_{\mathrm{s0}}+L_{\sigma\Delta}\right)}\left(i_{\mu\mathrm{a}}+i_{\mu\mathrm{c}}\right) \\ i_{\mathrm{C}} = \dfrac{2L_{\sigma}+2L_{\mathrm{s0}}+3L_{\sigma\Delta}}{3\left(L_{\sigma}+L_{\mathrm{s0}}+L_{\sigma\Delta}\right)} i_{\mu\mathrm{c}} - \dfrac{L_{\sigma}+L_{\mathrm{s0}}}{3\left(L_{\sigma}+L_{\mathrm{s0}}+L_{\sigma\Delta}\right)}\left(i_{\mu\mathrm{a}}+i_{\mu\mathrm{b}}\right) \end{cases} \tag{13}$$

Where i_{Δ} is the Δ-side circulating current, i_{A}, i_{B}, i_{C}, respectively, for the three-phase current, L_{σ}, $L_{\sigma\Delta}$ for the primary and secondary side of the leakage inductance Therefore, for the Yy wiring mode of the transformer, there is almost no electrical or magnetic interactions between the phases, and thus the excitation current of each phase is only based on the attenuation of the respective circuit parameters. That is, the rate of decay of the excitation current is positively related to the size of the current. As for the transformer with Yd11 wiring, due to the loop current on the Δ-side, the excitation current of a phase not only flows through the circuit of this phase, but also through the circuits of the other two phases, and is attenuated by the parameters of the other two phases. From the above analysis, it can be seen that the Yd11 transformer is affected by the Δ-side loop current when the flux linkage is saturated, and the decay rate of each phase current affects each other, resulting in the original faster decaying current decaying slower, and the slower decaying current decaying faster, which narrows down the difference in the decay rate of each phase current.

Since it is not possible to get the current on the Δ-side accurately, the differential current of Yd11 transformer is calculated in practice by using the compensation method of phase-to-phase differential, so the differential current of each phase is

$$\begin{cases} i_{\mathrm{dA}} = \dfrac{1}{\sqrt{3}}\left(i_{\mathrm{A}}-i_{\mathrm{B}}\right)-i_{a} \\ i_{\mathrm{dB}} = \dfrac{1}{\sqrt{3}}\left(i_{\mathrm{B}}-i_{\mathrm{C}}\right)-i_{b} \\ i_{\mathrm{dC}} = \dfrac{1}{\sqrt{3}}\left(i_{\mathrm{C}}-i_{\mathrm{A}}\right)-i_{c} \end{cases} \tag{14}$$

From Eq. 14, it can be seen that the per-phase differential current is the difference between the currents of the two phases, and thus the attenuation of the per-phase differential current is related to the impedance parameters of both phases. As shown in Fig. 9, due to the phase difference compensation, it results in a decrease in the rate of change of the originally fast change and an increase in the rate of change of the slow change. The difference in the rate of change of the current changes in each phase is reduced.

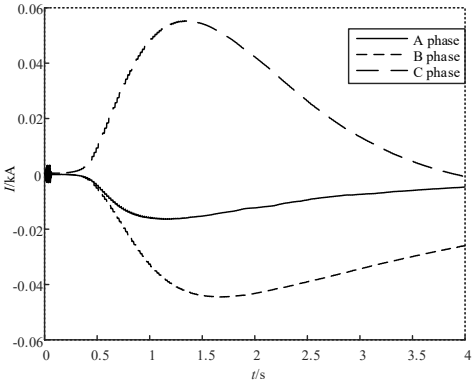

(a) Yy wiring transformer

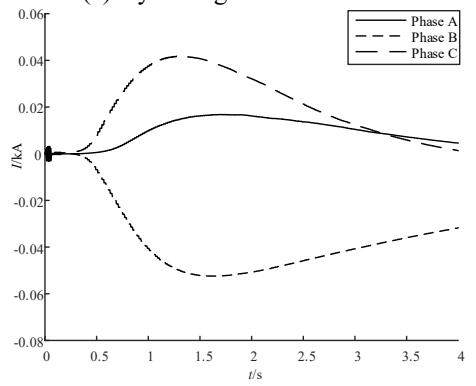

(b) Yd11 wiring transformer

Fig. 9 Circuit of the attenuation trend of the sympathetic inrush current non-periodic components

In summary, Yd11 transformer has little difference in attenuation rate between differential currents due to Δ-side circulating currents as well as phase difference compensation, while the occurrence of internal faults results in lower attenuation constants due to parameter changes in the faulted phase. Therefore, it is possible to ensure that the occurrence and sympathetic inrush currents are not inadvertent by comparing the non-periodic component attenuation rates of the differential currents.

4.2 Non-periodic component-based CT saturation detection technique

According to the analysis of the differential protection misoperation above, the primary current's prolonged non-periodic component in the sympathetic inrush current causes CT saturation, which in turn causes this abnormal misoperation. The error current brought on by CT saturation makes up the majority of the differential current in this instance, and the harmonic component is comparatively small. This section proposes a novel CT saturation detection algorithm by analyzing the mechanism of CT saturation associated with this type of error, as the conventional second harmonic criterion fails to effectively prevent such errors. There are two phases to the CT saturation process: 1) Following the generation of the sympathetic

inrush current, the nonperiodic component enters the current transformer, where the current transformer is not yet saturated and the differential current is comparatively low. Simultaneously, the CT core experiences an increase in error current due to the nonperiodic component of the current. Since the CT is not yet saturated, the excitation current in the CT is still low even though the CT iron core produces an increasing bias flux. 2) The flux in the CT iron core is almost saturated as the bias flux builds up, but the secondary side is still unsaturated. The inductance is kept at a comparatively low value by the periodic component's low amplitude, which confines the flux to a local hysteresis loop close to the saturation point. A local transient saturation is produced and harmonic discrimination is impacted as a result of the differential current having a periodic component with sizable non-periodic components. Saturation of the CT core causes the excitation inductance to drop quickly, allowing the non-periodic component to pass through the excitation branch and, ultimately, significantly lowering the non-periodic component in the transmitted differential current. The above analysis reveals that CT saturation leads to a reduction in the nonperiodic component of the differential current and proposes a corresponding saturation detection principle, and only single-phase CT saturation is analyzed in this section.

Define the non-periodic component of the current transformer transmitted current

$$I_{\mathrm{dc,m}}(n)=\frac{1}{N}\sum_{j=0}^{N-1}i_k(n-j),\mathrm{m}=1,2 \tag{15}$$

where N is the sampling point per cycle and the subscript m is the primary and secondary side CT currents. $I_{\mathrm{dc,m}}(n)$ is the value computed for the nth sampling point. Define the non-periodic component variation of CT transmission current.

$$S_{\mathrm{m}}(n)=\left\{\left[I_{\mathrm{dc,m}}(n)-I_{\mathrm{dc,m}}(n-i)\right]-\left[I_{\mathrm{dc,m}}(n-i)-I_{\mathrm{dc,m}}(n-2i)\right]\right\}\mathrm{m}=1,2 \tag{16}$$

In this work, i is set to $N/8$, where i is an integer. When both sides of the element exhibit a higher non-periodic component of the current transmitted by the CT, it is believed that the CT may enter a saturated state. Under typical circumstances, CT saturation detection is in a normal state.

$$\left(|I_{\mathrm{dc,1}}|>K_{\mathrm{set1}}|\dot{I}_1|\right)\&\left(|I_{\mathrm{dc,2}}|>K_{\mathrm{set1}}|\dot{I}_2|\right)\&(I_{\mathrm{d}}<I_{\mathrm{dset}}) \tag{17}$$

where I_{dset} is the action's corrected value and K_{set1} is set to 0.2 in this study, $\dot{I}_1$ and $\dot{I}_2$ are the current phases transmitted by the primary and secondary CTs, respectively, obtained by the FFT algorithm. The non-periodic component of the secondary side of the CT rapidly drops when the differential protection approaches the braking zone; this differential current is most likely the result of the CT becoming saturated. Consequently, the next judgmental step will be executed,

$$(S_1>S_{\mathrm{set}}>S_2)\&(|I_{\mathrm{dc,1}}|<K_{\mathrm{set2}}|I_{\mathrm{dc,1}}|)\&(I_{\mathrm{d}}<I_{\mathrm{dset}}) \tag{18}$$

where K_{set2} is set to 0.8 in this paper and S_{set} is the threshold value of the amount of change, S_1 and S_2 variations in the non-periodic component of the current

transmitted by the primary and secondary CTs. Eq. 18 shows that the CT non-periodic component on the secondary side of the transformer starts to decay less than that on the primary side.

$$(|I_{dc,2}|<K_{set1}|I_{dc,1}|)\&(S_1<S_{set})\&(I_d>I_{dset}) \tag{19}$$

At this point, the non-periodic component of CT on the transformer's secondary side decays to nearly zero, according to Eq. 19. Due to CT saturation on the secondary side of the transformer, the differential protection enters the action zone during this time, causing an incorrect action. The CT on the transformer's primary side is likewise subject to the aforementioned procedure. The CT typically goes through two cycles to reach the saturation condition. By raising the protection's action threshold and decreasing its action area, the protection mistake is prevented in the saturated state of CT. The enhancement scheme, as shown in Fig. 10, can effectively avoid and sympathetic inrush current-induced potential false-action risk of differential protection by increasing the differential protection action threshold value.

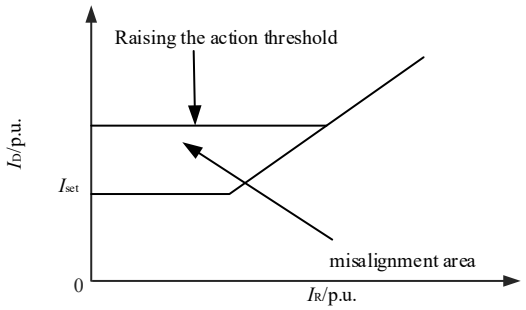

Fig. 10 Rasing up the pickup threshold value the differential characteristic

4.3 Protection program design

Define k as the non-periodic component of the differential current, and characterize the variation of the non-periodic component by the value dk obtained by dividing the difference of k by the period T.

$$dk(n)=\frac{k(n)-k(n-N)}{T} \tag{20}$$

Where: N is the number of sampling points per cycle; k (n) is the value of the non-periodic component calculated in the nth sampling point and T is the industrial frequency period.

The criterion based on the rate of change of k is as follows:

The threshold value is determined by the transformer's real condition, and the sympathetic inrush current is identified when dk>kth1 and dk<kth2 are continuously satisfied during the sampling period. This criterion is matched with the second harmonic criterion and utilized as an auxiliary criterion for the second

harmonic. In conclusion, Fig. 11 illustrates the protection plan suggested in this research using the reasoning that follows:

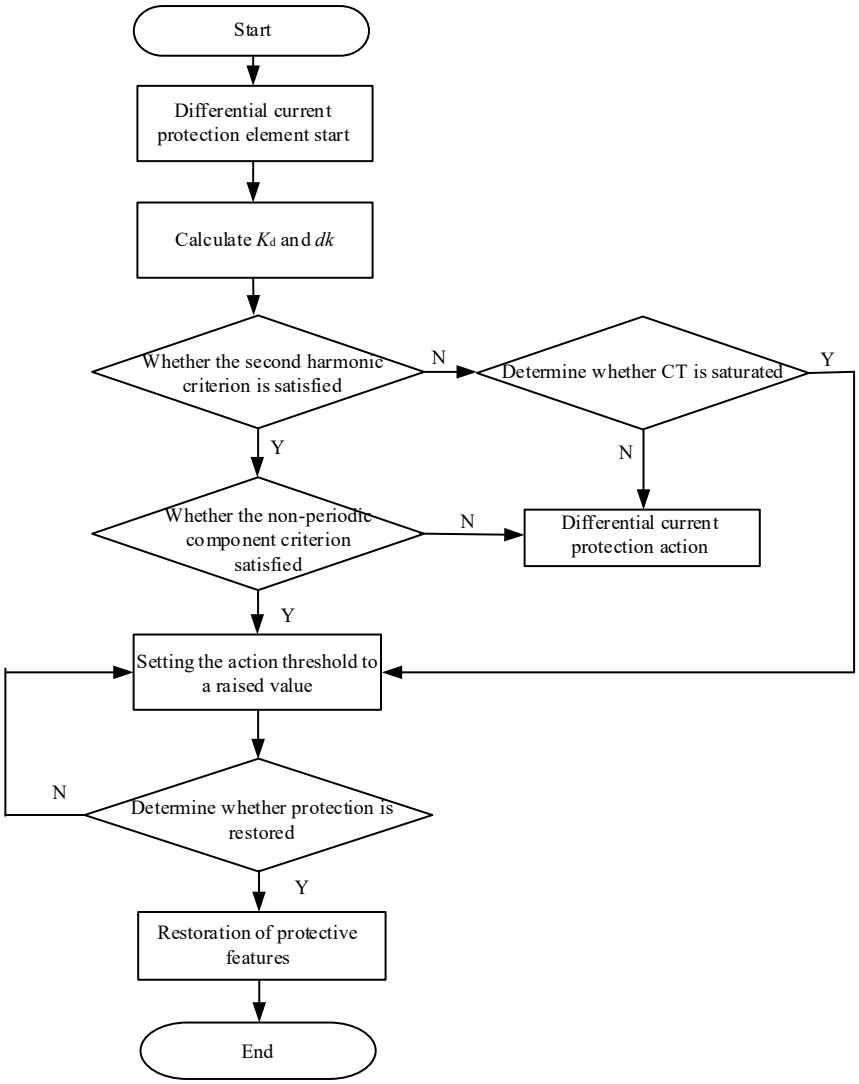

Fig. 11 Flowchart of the sympathetic inrush identification method

(1) First, when the differential protection element is activated, the second harmonic percentage and the rate of change of non-periodic variables are calculated. If the second harmonic braking and non-periodic component criterion are satisfied, the inrush current is judged to occur.

(2) During the period when the second harmonic braking is not satisfied, calculate the change of the non-periodic component on the secondary side of the CT to determine whether the criterion of CT saturation is satisfied, and if the

criterion is satisfied, raise the action threshold. If the criterion is not satisfied, the differential protection is operated.

(3) When identifying a sympathetic interaction, precautions should be taken to reduce the possibility of a protection malfunction while also guaranteeing the protection of internal faults. This can be achieved by raising the protection's action threshold and lowering its action area until the following circumstances are satisfied and the differential protection threshold reverts to its initial value. 1. The running transformer's differential current is consistently lower than the initial differential protection's current action level. 2. After entering initially in the action area, the transformer is launched.

5. Simulation Verification

As seen in Fig. 4, a shunt transformer simulation model is established in this research using PSCAD. Using the specifications of a converter transformer of a converter station, the criterion values are set to k_{th1}=5, k_{th2}=50. The rated capacity is 283.3MVA, the rated voltage is 525kV/290.88kV, the primary and secondary side resistance specifications are 0.002p.u., the leakage inductance is 0.1p.u., the system impedance is R_s=10Ω, and L_s=0.3H.

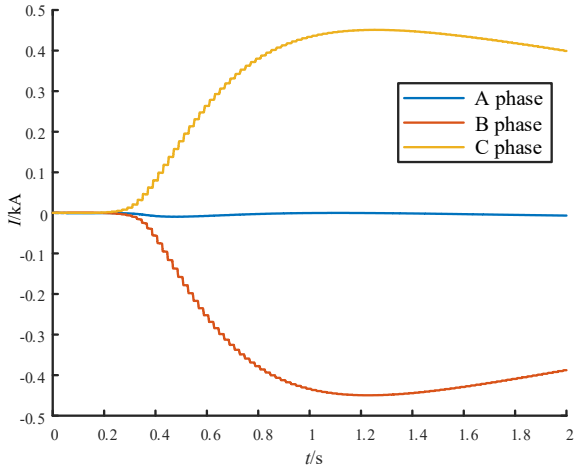

(a) sympathetic inrush current non-periodic components

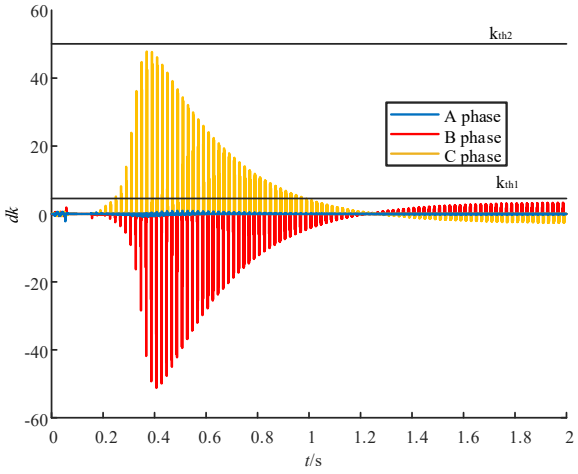

(b) *dk* of sympathetic inrush current

Fig. 12 The non-periodic components and the variation of dk during the sympathetic inrush identification

As shown in Fig. 12(a), after T_2 is closed, T_1 flux linkage is gradually saturated and the non-periodic component starts to increase, and the calculated rate of change of the non-periodic component is shown in Fig. 12(b), which satisfies the criterion for at least two cycles after the occurrence of the sympathetic inrush current. And when turn-to-turn short circuit occurs, as shown in Fig. 13, the maximum value of *dk* exceeds k_{th2} in the first cycle, after which the nonperiodic component rapidly decreases to below k_{th1}, recognizing that an internal turn-to-turn short circuit occurs, and the protection operates.

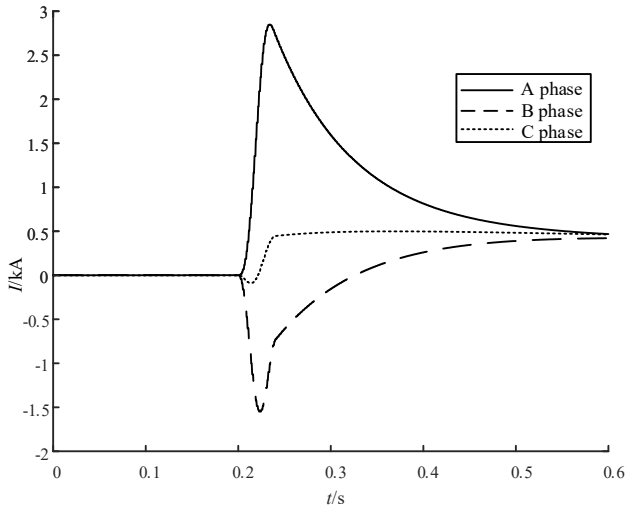

(a) Turn-to-turn short circuit non-periodic component

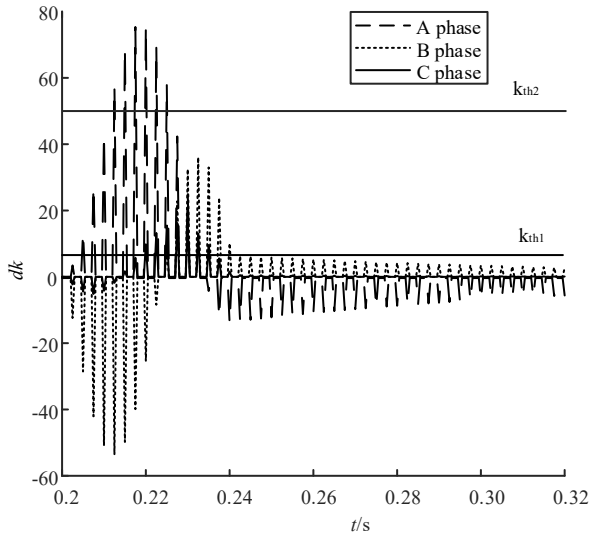

(b) *dk* of turn-to-turn short circuit

Fig. 13 The non-periodic components and the variation of dk during the Inter-turn short circuit

Fig. 14 shows the process of identifying CT saturation, where the nonperiodic component appears in the CT at 0.2s. Satisfying Eq.17, the CT method proceeds to the next step. At 0.41s, it starts to decrease and in the next 50ms, it decreases to almost zero as the differential current increases. During this period, Eq. 18 and Eq. 19 are judged to determine whether the CT enters the saturation state to prevent false activation.

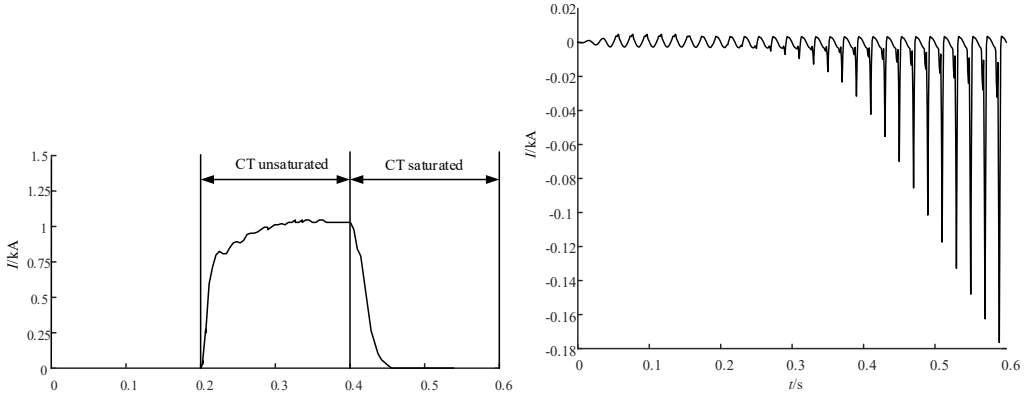

(a) Non-periodic component of CT (b) sympathetic inrush current

Fig. 14 CT saturation process

6. Conclusions

The mechanism and change features of the sympathetic inrush current are examined in this work, along with the properties of the current and its identification

method. It is discovered that the non-periodic component of the inrush current causes the current transformer to temporarily become saturated, which lowers the differential current's second harmonic content and causes protection to malfunction. In addition to the possibility of a turn-to-turn short circuit, protection refusal will occur if the second harmonic content exceeds the braking factor. According to the various decay speeds of the non-periodic component of the differential current during the occurrence of the sympathetic inrush current and turn-to-turn short circuit, as well as the non-periodic component of the current transmitted in the process of CT saturation, this paper suggests a method of identifying the sympathetic inrush current based on the change characteristics of the non-periodic component as an auxiliary criterion for second harmonic braking. It then optimizes the traditional differential protection and confirms that the sympathetic inrush current can be accurately identified through simulation. It is verified by simulation that the sympathetic inrush current can be recognized quickly.

Acknowledgment

This work is supported by the Science and Technology Project of State Grid Jibei Electric Power Co., Ltd. UHV Branch (Contract No. SGJBJX00JLJS2400786).

R E F E R E N C E S

[1]. Wang Y, Qi X, Yin X, et al. Identification and coping approaches of sympathetic inrush current based on the station-area information of smart substation//2015 5th International Conference on Electric Utility Deregulation and Restructuring and Power Technologies (DRPT). IEEE, 2015: 1020-1024.

[2]. Nadhirah N F, Halim H A, Hussin N, et al. Mitigation on sympathetic inrush current phenomena between parallel-connected transformers using PSCAD/EMTDC//2022 IEEE International Conference on Power Systems Technology (POWERCON). IEEE, 2022: 1-6.

[3]. YAHIOU A, BAYADI A, BABES B. Mitigation of sympathetic inrush current in transformer using the technique of point on voltage wave control switching//2018 International Conference on Communications and Electrical Engineering (ICCEE). IEEE, 2018: 1-6.

[4]. Richter M, Mehlmann G, Luther M. Impact of recovery and sympathetic inrush phenomena on VSC HVDC systems//2022 57th International Universities Power Engineering Conference (UPEC). IEEE, 2022: 1-6.

[5]. Nadhirah N F, Halim H A. Effect of Load Capacitance on Sympathetic Inrush Current//2023 International Conference on Technology and Policy in Energy and Electric Power (ICT-PEP). IEEE, 2023: 305-309.

[6]. HAYWARD C D. Prolonged inrush currents with parallel transformers affect differential relaying J. Transactions of the American Institute of Electrical Engineers,2013, 60(12):1096-1101

[7].Pan Y, Yin X, Yin X, et al. Zero-Mode Inrush Current Characteristics and Zero-Sequence Protection Countermeasure Under Sympathetic Interaction. IEEE Transactions on Power Delivery, 2021, 37(5): 3669-3678.

[8]. Jin M, Yin X, You D. Reason of differential protection mal-operation caused by complex sympathetic inrush and its countermeasure. Proceedings of the CSEE, 2011, 31(1): 86-93.
[9]. Shao D, Yin X, Zhang Z, et al. Method to identify transformer sympathetic inrush based on the fundamental component increment. Proceedings of the CSEE, 2010, 30(10): 78-83.
[10]. Zheng T, Gu J, Huang S F, et al. A new algorithm to avoid maloperation of transformer differential protection in substations with an inner bridge connection. IEEE Transactions on Power Delivery, 2012, 27(3): 1178-1185.
[11]. Mahmoudian Y, Sanati S, Allameh A, et al. The effect of sympathetic inrush current on the protection maloperation in the capacitor feeder at Shahroud 63kV substation//2020 15th International Conference on Protection and Automation of Power Systems (IPAPS). IEEE, 2020: 80-83.
[12]. Medeiros R P, Costa F B. A wavelet-based transformer differential protection: Internal fault detection during inrush conditions. IEEE Transactions on Power Delivery, 2018, 33(6): 2965-2977.
[13]. Cimadevilla R. Inrush currents and their effect on protective relays//2013 66th Annual Conference for Protective Relay Engineers. IEEE, 2013: 467-504.
[14]. Rudez U, Mihalic R. A reconstruction of the WAMS-detected transformer sympathetic inrush phenomenon. IEEE Transactions on Smart Grid, 2016, 9(2): 724-732.
[15]. Li R, Song S, Ma Z, et al. A simulation study of the influence of magnetizing inrush current and sympathetic inrush current of converter transformers//2016 IEEE PES Asia-Pacific Power and Energy Engineering Conference (APPEEC). IEEE, 2016: 2282-2286.
[16]. Kahraman K T, Ozgonenel O. An ANN-wavelet based distribution transformer protection//IET Conference Proceedings CP878. Stevenage, UK: The Institution of Engineering and Technology, 2024, 2024(3): 1-7.
[17]. Ahmadzadeh-Shooshtari B, Rezaei-Zare A. Advanced transformer differential protection under GIC conditions. IEEE Transactions on Power Delivery, 2021, 37(3): 1433-1444.
[18]. Jaworski M, Jaeger J. Sympathetic transformer inrush detection and relay blocking during power system restoration. IEEE Transactions on Power Delivery, 2023, 38(4): 2408-2417.
[19]. Wang F, Qi X, Wang Y, et al. A sympathetic inrush detection method based on on-line magnet flux calculation//2014 International Conference on Power System Technology. IEEE, 2014: 700-704.
[20]. Qi X, Yin X, Zhang Z. sympathetic inrush current in a transformer and a method for its identification. IEEJ Transactions on Electrical and Electronic Engineering, 2016, 11(4): 442-450.